DCFoil Developer and User Documentation

Galen W. Ng

January 30, 2024

Summary

DCFoil is a program for the dynamic analysis and design optimization of composite hydrofoils.

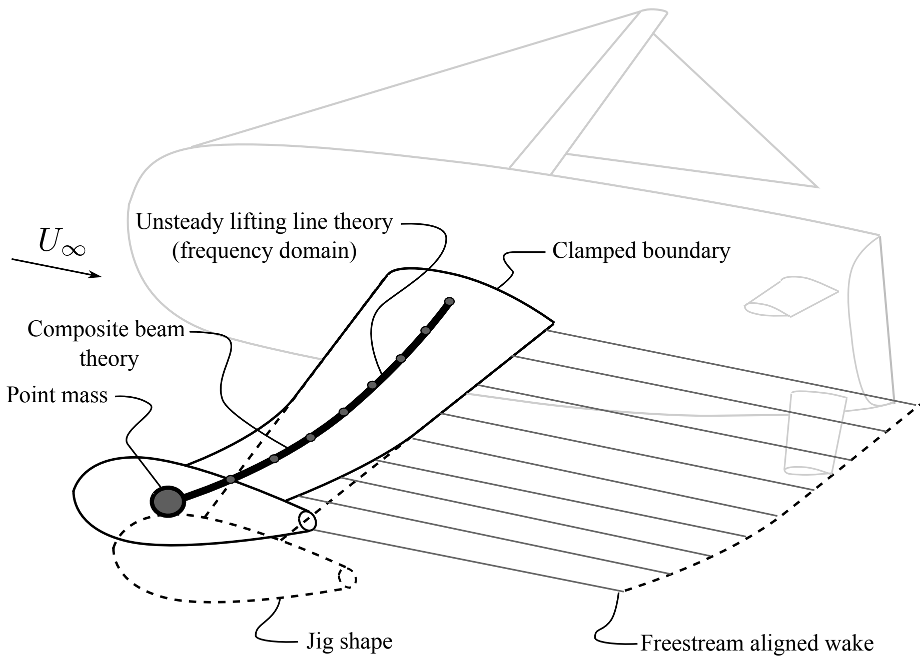

Figure 1: DCFoil modeling approach

Contents

1 Coordinate system **3**

2 Discretization **4**
2.1 Structural model . . . 4
2.1.1 Beam finite element . . . 4
2.1.2 Beam parameters for composite materials via CLT . . . 4
2.1.3 Structural damping . . . 5
2.2 Hydrodynamic loads . . . 5
2.2.1 Steady lifting line . . . 5
2.2.2 Extension to unsteady frequency domain . . . 6

3 Static solution **8**

4 Forced vibration solution **9**
4.1 Governing equations . . . 9

5 Flutter solution **10**
5.1 Governing equations . . . 10
5.2 Mode tracking . . . 10
5.3 Mode space reduction . . . 11
5.4 Cost functions . . . 12
5.4.1 Flutter . . . 12
5.4.2 Coalescence . . . 12

6 Rigid body dynamics **12**
6.1 Governing equations . . . 12
6.2 Kinematics . . . 12
6.3 Inertia . . . 12
6.4 Equations of motion . . . 13
6.4.1 Gravitational loads . . . 13
6.4.2 Propulsive forces . . . 13
6.4.3 Hydrodynamic loads . . . 13
6.4.4 Elastified equations of motion . . . 13

1 Coordinate system

Flow is in the x-direction, span is in the y-direction, and the vertical direction is z.

2 Discretization

2.1 Structural model

The local beam model uses the spanwise direction as x (subscript 1), the chordwise direction as y (subscript 2), and the vertical direction as z (subscript 3). It is transformed to the global coordinate system by the rotation matrices.

2.1.1 Beam finite element

The composite beam model uses the well-known slender beam parameters EI_s, GJ_s, EA_s, and additionally S_s and K_s to account for structural warping of non-circular cross sections and material bend-twist coupling, respectively. No axial coupling to other degrees of freedom (DOF) is currently considered. The beam is discretized into 2-noded elements with 9 displacement DOFs denoted u, v, w, ϕ, θ, ψ, ϕ', θ', ψ'.

2.1.2 Beam parameters for composite materials via CLT

The beam parameters are computed from classical lamination theory (CLT) for composite plates using the high aspect ratio plate model from Weisshaar and Foist [1].

$$EI = c\left(D_{11} - \frac{D_{12}^2}{D_{22}}\right), \quad GJ = 4c\left(D_{66} - \frac{D_{26}^2}{D_{22}}\right), \quad K = 2c\left(D_{16} - \frac{D_{26}D_{12}}{D_{22}}\right) \tag{1}$$

These relations do not restrict chordwise rigidity (camber), but they do assume zero chordwise moment. Lottati [2] used the chordwise rigid relations, which simplifies the algebra.

The flexural stiffnesses D_{ij} (6x6 matrix) come via CLT

$$D_{11} = Q_{11}\cos^4(\theta_f) + 2\left(Q_{12} + 2Q_{66}\right)\sin^2(\theta_f)\cos^2(\theta_f) + Q_{22}\sin^4(\theta_f) \tag{2}$$

$$D_{22} = Q_{11}\sin^4(\theta_f) + 2\left(Q_{12} + 2Q_{66}\right)\sin^2(\theta_f)\cos^2(\theta_f) + Q_{22}\cos^4(\theta_f) \tag{3}$$

$$D_{66} = \left(Q_{11} + Q_{22} - 2Q_{12} - 2Q_{66}\right)\sin^2(\theta_f)\cos^2(\theta_f) + Q_{66}\left(\sin^4(\theta_f) + \cos^4(\theta_f)\right) \tag{4}$$

$$D_{12} = \left(Q_{11} + Q_{22} - 4Q_{66}\right)\sin^2(\theta_f)\cos^2(\theta_f) + Q_{12}\left(\sin^4(\theta_f) + \cos^4(\theta_f)\right) \tag{5}$$

$$D_{16} = \left(Q_{11} + Q_{22} - 2Q_{66}\right)\sin(\theta_f)\cos^3(\theta_f) + \left(Q_{12} - Q_{22} + 2Q_{66}\right)\sin^3(\theta_f)\cos(\theta_f) \tag{6}$$

$$D_{26} = \left(Q_{11} + Q_{22} - 2Q_{66}\right)\sin^3(\theta_f)\cos(\theta_f) + \left(Q_{12} - Q_{22} + 2Q_{66}\right)\sin(\theta_f)\cos^3(\theta_f) \tag{7}$$

The reduced in-plane stiffness coefficients Q_{ij} for the individual plies are

$$Q_{11} = \frac{E_1}{1 - \nu_{12}\nu_{21}}, \quad Q_{12} = \frac{\nu_{12}E_2}{1 - \nu_{12}\nu_{21}}, \quad Q_{22} = \frac{E_2}{1 - \nu_{12}\nu_{21}}, \quad Q_{66} = G_{12} \tag{8}$$

The following are numerical methods for computing structural properties of airfoils. The sectional mass properties are

$$m_s = \int_0^c \rho\left(Z_u - Z_\ell\right) dx \doteq \text{kg-m}^{-1} \tag{9}$$

$$I_s = \int_0^c \int_0^{t_{\max}} r^2 dm \tag{10}$$

where we evaluate the integrals numerically.

The sectional geometric properties are[1]

$$\bar{z} = \frac{1}{A}\int_0^c \frac{1}{2}\left[Z_u^2 - Z_\ell^2\right] dx \tag{11}$$

$$I = \int_0^c \frac{1}{3}\left[(Z_u - \bar{z})^3 - (Z_\ell - \bar{z})^3\right] dx \tag{12}$$

$$J = \int \tag{13}$$

$$\tag{14}$$

[1]The torsional constant is NOT the same as the polar moment

and torsional warping resistance due to tension from Lottati [2] is

$$S = \int_{-b}^{b} D_{22} x_a^2 dx, \quad \text{where } x_a = x - ba \tag{15}$$

2.1.3 Structural damping

We use a proportional (Rayleigh) damping model, which is commonly used for multi-DOF structures because of mathematical conveniences

$$\mathbf{C_s} = \alpha \mathbf{M_s} + \beta \mathbf{K_s}.$$

The mass proportional damping decreases with increasing response frequency whereas the stiffness proportional damping increases. We specify $\zeta = 2\%$ damping ratio at an undamped, in-vacuum, natural frequency giving $\beta = 2\zeta/\omega_{\max}$ where $\omega_{\max}$ is the highest undamped, in-vacuum, natural frequency in radians per second determined from modal analysis–in this paper, the fourth natural mode.

A few options are available but we typically use the stiffness proportional method ($\alpha = 0$) because response frequencies in water tend to be on the lower side; we want to avoid artificial overdamping of critical hydroelastic modes with $\omega < \omega_{\max}$. Structural damping is typically small compared to hydrodynamic damping so its main role is as a margin of stability if fluid damping is close to zero, thus accuracy of the structural damping model is not critical.

2.2 Hydrodynamic loads

2.2.1 Steady lifting line

The lifting line model derives from Glauert [3, Ch. XI] and works for arbitrary chord. Specifically, we are after sectional lift slopes ($c_{\ell_\alpha} = dc_\ell/d\alpha = a_0$). We assume

- the chord is small compared to the span,
- the wing is symmetric about the centerline,
- span is straight and orthogonal to the freestream
- trailing vortices are shed from the trailing edge and align with the freestream (no sweep or dihedral)

The wing is represented by superimposing "horseshoe" systems of vortex lines (analagous to a wire with electrical current). This is because the circulation across a wing is not constant. The free vortex system is a sheet of trailing vortices springing from the trailing edge. The induced velocity of an element of the line (ds) at point P from one vortex line of constant strength Γ is

$$dq = \frac{\Gamma}{4\pi r^2} \sin(\theta) ds \tag{16}$$

but in practice, one would solve this is an integral over the entire vortex line, so we will build up to the full wing.

To begin solution, we first assume the circulation is the Fourier series[2]

$$\Gamma(y) = 2U_\infty s \sum_{n=1}^{\infty} a_n \sin(n\theta) \quad \text{where } y = -\frac{s}{2}\cos(\theta) \quad \text{and } \theta \in \left[-\frac{\pi}{2}, \frac{\pi}{2}\right]. \tag{17}$$

The difficulty is now determining the Fourier coefficients a_n so we need some relations for $\Gamma(y)$ to solve it.

One relation is the equation for the normal induced velocity (downwash velocity) at a point along the span

$$w(y) = \frac{1}{4\pi} \int_{-s/2}^{s/2} \frac{\frac{d\Gamma}{d\eta}}{y - \eta} d\eta = \boxed{-U_\infty \sum_{n=1}^{\infty} \frac{n a_n \sin(n\theta)}{\sin(\theta)}} \tag{18}$$

where η is the spanwise coordinate and s is total span. We skipped a few steps in the derivation [4, Sec. 3.7].

[2] Kerwin and Hadler [4] use $\tilde{y}$ as θ

The second relation is from sectional lift as a function of circulation. Recall that the circulation at a section (derived from Kutta-Joukowski lift theorem) is

$$\Gamma(y) = \frac{1}{2} c_\ell c U_\infty = \frac{1}{2} a_0 c \left(U_\infty \alpha - w(y)\right) \tag{19}$$

where we made use of $c_\ell = a_0 \alpha_{\text{eff}} = a_0 \left(\alpha - w/U_\infty\right)$. After substitution of the Fourier series form and combining Equations (18) and (19), we end up with

$$\sum_{n=1}^{\infty} a_n \sin(n\theta) \left(n\mu + \sin(\theta)\right) = \mu\alpha \sin(\theta) \quad \text{where } \mu(\theta) = \frac{a_0 c(\theta)}{4s} \tag{20}$$

Here's the digestion of the Julia code which does the numerical solution of Equation (20) but symmetrically about the centerline.

$$\begin{aligned}
&\tilde{y} = \left[0, \frac{\pi}{2}\right] \quad \text{of size nNodes} \\
&\mathbf{n} = [1 : 2 : 2 \times \text{nNodes}] \\
&\mathbf{c} = c \sin(\tilde{y}) \quad \text{(parametrized vector leading to elliptical planform)} \\
&\mathbf{b} = \frac{\pi}{4} \frac{\mathbf{c}}{s/2} \alpha \sin(\tilde{y}) \quad \text{(RHS of Equation (20) in vector form)} \\
&\tilde{y}n = \tilde{y} \otimes \mathbf{n} \quad \text{(outer product)} \\
&\mathbf{A_0} = \begin{bmatrix} | & | & \\ \sin(\tilde{y}) & \sin(\tilde{y}) & \cdots \\ | & | & \end{bmatrix} \quad \text{(square matrix of } \sin(\tilde{y})\text{)} \\
&\mathbf{A_1} = \frac{\pi}{4} \frac{\mathbf{c}}{s/2} \otimes \mathbf{n} \quad \text{(outer product representing } n\mu \text{ on LHS)} \\
&\mathbf{A} = \sin(\tilde{y}n) \odot (\mathbf{A_0} + \mathbf{A_1}) \\
&\mathbf{Ax} = \mathbf{b} \quad \text{(solve linear system for } \mathbf{x} = a_n\text{)} \\
&\Gamma(y) = 4U_\infty s/2 \left(\underbrace{\sin(\tilde{y}n)\mathbf{x}}_{\text{mat-vec product}} \right) \\
&c_\ell = \frac{2\Gamma(y)}{U_\infty c} \\
&c_{\ell_\alpha} = \frac{c_\ell}{\alpha}
\end{aligned}$$

2.2.2 Extension to unsteady frequency domain

We are interested in the sectional lift and moments for a harmonically oscillating body. Theodorsen [5] came up with the Theodorsen function $C(k)$ to account for the lag and deficit in forces with a farfield boundary condition. It is applied as a transfer function to the static hydrodynamics.

$$\begin{Bmatrix} F_z \\ M_y \end{Bmatrix}_i = -\left(\left[\mathbf{m_f} \begin{Bmatrix} \ddot{w} \\ \ddot{\psi} \end{Bmatrix}\right]_i + \left[\mathbf{c_f} \begin{Bmatrix} \dot{w} \\ \dot{\psi} \end{Bmatrix}\right]_i + \left[\mathbf{k_f} \begin{Bmatrix} w \\ \psi + \alpha_0 \end{Bmatrix}\right]_i + \left[\mathbf{\hat{c}_f} \begin{Bmatrix} \dot{w}' \\ \dot{\psi}' \end{Bmatrix}\right]_i + \left[\mathbf{\hat{k}_f} \begin{Bmatrix} w' \\ \psi' \end{Bmatrix}\right]_i \right) \Delta y_i \tag{21}$$

where Δy_i is the strip width at node i, which we assume to be equal to element length.

$$\mathbf{m_f} = \pi \rho_f b^2 \begin{bmatrix} 1 & ab \\ ab & b^2 \left(\frac{1}{8} + a^2\right) \end{bmatrix} \tag{22}$$

$$\mathbf{c_f}(k) = \frac{1}{2} \rho_f b U_0 \left(\cos(\Lambda) \begin{bmatrix} c_{\ell_\alpha} 2C(k) & -b \left[2\pi + c_{\ell_\alpha}(1 - 2a)C(k)\right] \\ c_{\ell_\alpha} eb2C(k) & \frac{b}{2}(1 - 2a)(2\pi b - c_{\ell_\alpha} 2ebC(k)) \end{bmatrix} \right) \tag{23}$$

$$\mathbf{k_f}(k) = \frac{1}{2}\rho_f U_0^2 \cos(\Lambda) \left(\cos(\Lambda) \begin{bmatrix} 0 & -C(k)2bc_{\ell_\alpha} \\ 0 & -2eb^2 c_{\ell_\alpha} C(k) \end{bmatrix} \right) \tag{24}$$

$$\hat{\mathbf{c}}_\mathbf{f}(k) = \frac{1}{2}\rho_f b U_0 \sin(\Lambda) \left(\begin{bmatrix} 2\pi b & 2\pi a b^2 \\ 2\pi a b^2 & 2\pi b^3 \left(\frac{1}{8} + a^2\right) \end{bmatrix} \right) \tag{25}$$

$$\hat{\mathbf{k}}_\mathbf{f}(k) = \frac{1}{2}\rho_f b U_0 \sin(\Lambda) \left(U_0 \cos(\Lambda) \begin{bmatrix} c_{\ell_\alpha} 2C(k) & -c_{\ell_\alpha} b(1-2a)C(k) \\ 2ebc_{\ell_\alpha} C(k) & \pi b^2 - c_{\ell_\alpha} e b^2 (1-2a) C(k) \end{bmatrix} \right) \tag{26}$$

The extra $\hat{\square}$ matrices account for sweep effects on the quasi-steady (damping and stiffness) aerodynamics and are lumped into their respective global matrices if they are in phase with velocity or displacements.

3 Static solution

4 Forced vibration solution

4.1 Governing equations

The frequency response solver separates the magnitudes of static and fluctuating parts of the solution $\mathbf{u_{tot}} = \mathbf{u_{dyn}} + \mathbf{u_{stat}}$. The static problem is solved the same way as previously described in, and we solve the dynamic part using the second-order dynamic governing equations for the user-prescribed harmonic forcing vector in the Laplace domain. We use $j = \sqrt{-1}$. Equation becomes

$$\underbrace{\left(-\omega^2\left(\mathbf{M_f} + \mathbf{M_s}\right) + j\omega\left(\mathbf{C_f} + \mathbf{C_s}\right) + \left(\mathbf{K_f} + \mathbf{K_s}\right)\right)}_{\mathbf{D}(\omega)}\tilde{\mathbf{u}} = \tilde{\mathbf{f}}. \tag{27}$$

In this case, we substituted $\mathbf{u_{dyn}} = \tilde{\mathbf{u}}e^{j\omega t}$ and $\mathbf{f_{ext,dyn}} = \tilde{\mathbf{f}}e^{j\omega t}$ into since we are looking at forced harmonic vibration, and we care more about the steady-state (particular) solution than the initial transience (complementary solution). The system dynamic matrix ($\mathbf{D}(\omega)$), also known as the *impedance matrix*, is not symmetric because of the fluid governing equations. We solve for the dynamic response with direct inversion of the dynamic matrix. We solve this equation for a sweep of forcing frequencies ($f = \omega/(2\pi)$) and then compute the frequency response curves. The steady-state, frequency response is $\tilde{\mathbf{u}} = \mathbf{D}^{-1}\tilde{\mathbf{f}}$.

The inverse matrix $\mathbf{H}(\omega) = \mathbf{D}^{-1}(\omega)$ is the RAO or frequency response function (FRF), and it is an nDOF×nDOF matrix computed for every exciting frequency ω. Knowing the RAO is extremely important for understanding foil response to dynamic loading such as from waves or cavity shedding.

5 Flutter solution

5.1 Governing equations

The *p*-*k* method is commonly used in aeroelastic flutter predictions. The governing equation is solved by assuming a solution of the form $\mathbf{u} = \tilde{\mathbf{u}}e^{pt}$, where $p = \xi + jk$ is our non-dimensional complex eigenvalue, ξ is non-dimensional damping, and k is the reduced frequency. Eigenvalues are non-dimensionalized using $U_\infty \cos(\Lambda)/\bar{b}$ where $\bar{b}$ is the mean semi-chord. The generalized governing discrete equation takes the form

$$\left[\left(\frac{U_\infty \cos(\Lambda)}{\bar{b}}\right)^2 p_n^2 \left(\mathbf{M_s} + \mathbf{M_f}\right) + \frac{U_\infty \cos(\Lambda)}{\bar{b}} p_n \mathbf{C_s} + \mathbf{K_s} - \mathbf{f_{hydro,quasi}}\right] \tilde{\mathbf{u}}_n = \mathbf{0} \qquad \text{for } n = 1, \ldots, \text{nmode}. \quad (28)$$

where $\mathbf{f_{hydro,quasi}}$ are the quasi-steady hydrodynamic forces. For a non-trivial solution of $\tilde{\mathbf{u}}$, the flutter determinant $\det(\Delta)$ is zero, where the bracketed matrix in Equation (28) is Δ. We need to find the p's that satisfies the quadratic eigenproblem so that $\det(\Delta) = 0$. The corresponding $\tilde{\mathbf{u}}$ is then the complex eigenvector describing the flutter mode shape. Simulations sweep flow speed (U_∞). We can compute in-vacuum natural frequencies by setting all fluid matrices and total damping to zero, giving a linear eigenvalue problem with symmetric matrices; the eigenvector is the corresponding in-vacuum mode shape.

We can linearize the quadratic eigenvalue problem using the identity $\mathbf{I}\dot{\mathbf{u}} = \mathbf{I}\dot{\mathbf{u}}$ to obtain this linear, generalized eigenvalue problem

$$p_n \begin{bmatrix} \mathbf{I} & \mathbf{0} \\ \mathbf{0} & \left(\frac{U_\infty \cos(\Lambda)}{\bar{b}}\right)^2 \mathbf{M} \end{bmatrix} \begin{Bmatrix} \tilde{\mathbf{u}} \\ p_n \tilde{\mathbf{u}} \end{Bmatrix} - \begin{bmatrix} \mathbf{0} & \mathbf{I} \\ -\mathbf{K} & -\frac{U_\infty \cos(\Lambda)}{\bar{b}} \mathbf{C} \end{bmatrix} \begin{Bmatrix} \tilde{\mathbf{u}} \\ p_n \tilde{\mathbf{u}} \end{Bmatrix} = \mathbf{0}, \quad (29)$$

We solve Equation (29) following the method of van Zyl [6] since Jonsson [7] has shown the method is suitable and sufficiently robust enough for gradient-based optimization. The flutter solution method is

1. For a given velocity, solve the eigenvalue problem (Equation (29)) for a range of reduced frequencies k.
2. Eigenvalues (p) are valid roots if $\Im(p)$ matches the assumed k (matched point solution).
3. Monitor the difference $\Im(p) - k$. A change in sign indicates a root.
4. Determine the root by linear interpolation.

where we follow the methodology outlined in Jonsson et al. [8] and Jonsson [7, Ch. 3]. Since the linear system is quite large, we also use a mode space reduction technique commonly known as the *normal mode* (or modal) method to reduce the size of the matrices and computational cost.

5.2 Mode tracking

The mode tracking method prevents mode swapping or hopping during two stages of the flutter analysis:

1. during the reduced frequency sweep at a given flight condition and
2. during the dynamic pressure increments between flight conditions.

We employ the mode tracking method from van Zyl [9], which uses complex inner products between current and previous eigenvectors to populate a correlation matrix. $\tilde{\mathbf{C}}$. We search the matrix for largest elements (maximum of one) where the row and column denote previous iteration and current iteration, respectively. We do this for all modes. In the frequency sweep, building $\tilde{\mathbf{C}}$ is simpler because it is square as the number of eigenvectors between k iterations is the same, resulting in one-to-one mapping. Between dynamic pressure increments, modes can show up or disappear so $\tilde{\mathbf{C}}$ is rectangular. Therefore, we use a correlation metric (vector $\mathbf{c}$) to determine if the computed set of eigenvalues are too far from previously computed values, the process of which is outlined in Algorithm 1. Based on the correlation metric value, we either accept or reject the eigenvalues and eigenvectors. If they are rejected, the dynamic pressure step is halved and we re-run the reduced frequency sweep; however, the halving process is controlled by a minimum allowed increment $\Delta q_{\min}$ to prevent excessively long computation times. If $\Delta q_{\min}$ is reached, then we accept the roots.

Algorithm 1: Mode tracking between dynamic pressure increments $q^{(n)}$ and $q^{(n+1)}$ of Jonsson [7] adapted from van Zyl [9].

Data: Complex eigenvector matrix $\mathbf{V}^{(n)}$ and $\mathbf{V}^{(n+1)}$ at succesive q's of size $n_{\text{dof}} \times n_v^{(n)}$ and $n_{\text{dof}} \times n_v^{(n+1)}$
Result: Vector $\mathbf{c}$ of size $n_v^{(n+1)}$ and array $\mathbf{m}$ of size $2 \times n_v^{(n+1)}$
1 Compute $S_{3i} = ||\mathbf{v}_i^{(n)}||_2$ and $S_{4i} = ||\mathbf{v}_i^{(n+1)}||_2$;
2 Compute Hadamard product $\mathbf{C} = |\mathbf{V}^{(n)^H} \circ \mathbf{V}^{(n+1)}|$;
3 $\tilde{\mathbf{C}} = \mathbf{C}_{ij}/\left(S_{3i}S_{4j}\right)$;
4 Search $\tilde{\mathbf{C}}$ for maximum element;
5 Store row and column indices in array $\mathbf{m}$ and then the correlation values in $\mathbf{c}$;
6 Set the corresponding rows and columns in $\tilde{\mathbf{C}}$ to zero;
7 Repeat process until all elements in $\tilde{\mathbf{C}}$ are zero;

5.3 Mode space reduction

To reduce the problem size, we use mode space reduction to a reduced set of N_r generalized coordinates. The displacement field is approximated by

$$\mathbf{u} \approx \mathbf{Q}_r(y)\mathbf{q}(t) \tag{30}$$

where $\mathbf{q} \in \mathbb{R}^{N_r}$ is a vector of retained generalized coordinates and $\mathbf{Q}_r \in \mathbb{R}^{N_s \times N_r}$ is a matrix with columns corresponding to eigenvectors. This is typically called the normal mode method. One then solves the eigenvalue problem

$$\left(\mathbf{K_s} - \omega_i^2 \mathbf{M_s}\right)\bar{\mathbf{u}}_i = 0 \tag{31}$$

where ω_i is the natural frequency. We compute $\bar{\mathbf{u}}_i$ and collect them in the matrix

$$\mathbf{Q}_r = \begin{bmatrix} | & | & & | \\ \bar{\mathbf{u}}_1 & \bar{\mathbf{u}}_2 & \cdots & \bar{\mathbf{u}}_{N_r} \\ | & | & & | \end{bmatrix}. \tag{32}$$

Now the reduced stiffness and mass matrices are

$$\mathbf{M_s}_r = \mathbf{Q}_r^T \mathbf{M_s} \mathbf{Q}_r = \mathbf{I}_r \in \mathbb{R}^{N_r \times N_r} \tag{33}$$
$$\mathbf{K_s}_r = \mathbf{Q}_r^T \mathbf{K_s} \mathbf{Q}_r = \text{diag}\left[\omega_i^2\right] \tag{34}$$

and the governing equation reduces to

$$\mathbf{M_s}_r \ddot{\mathbf{q}} + \mathbf{C_s}_r \ddot{\mathbf{q}} + \mathbf{K_s}_r \mathbf{q} - \mathbf{Q}_r^T \mathbf{f}_{\text{hydro}} = \mathbf{0} \tag{35}$$

To apply this to the hydrodynamic loads, we obtain from Equation (**??**)

$$\mathbf{f}_{\text{hydro},r} = -\left(\mathbf{M_f}_r \ddot{\mathbf{u}} + \mathbf{C_f}_r \dot{\mathbf{u}} + \mathbf{K_f}_r \mathbf{u}\right) \tag{36}$$

where the matrices are

$$\mathbf{M_f}_r = \mathbf{Q}_r^T \mathbf{M_f} \mathbf{Q}_r \tag{37}$$
$$\mathbf{C_f}_r = \mathbf{Q}_r^T \mathbf{C_f} \mathbf{Q}_r \tag{38}$$
$$\mathbf{K_f}_r = \mathbf{Q}_r^T \mathbf{K_f} \mathbf{Q}_r. \tag{39}$$

Note, since cavitating flow leads to non-symmetric matrices, we cannot do all the simplifications Jonsson et al. [10] uses. TODO: OK, this is not actually true because we wouldn't be able to solve in the frequency domain...

5.4 Cost functions

Reverse mode algorithmic differentiation is applied on the upper-most flutter routine called `cost_funcs_with_derivs`

5.4.1 Flutter

The single flutter constraint uses the damping values ($g = \Re\{p\}$). We use a two-level KS function aggregation to compute the single constraint first used by Jonsson et al. [10]. It is

$$\mathrm{KS}_{\text{flutter}} = \mathrm{KS}\left(\mathrm{KS}\left(\Re\{p_{n,q}\}\right)\right) \tag{40}$$

where the first level is over all dynamic pressures $q = 1, \ldots, N_q$ and then over all modes $n = 1, \ldots, \text{nmodes}$. The KS function is

$$\mathrm{KS}(\mathbf{a}) = a_{\max} + \frac{1}{\rho} \ln \sum_i e^{\rho(a_i - a_{\max})} \tag{41}$$

where we set the aggregation parameter $\rho = 80$ by default.

5.4.2 Coalescence

6 Rigid body dynamics

The two coordinate systems are the *earth-fixed* and *body-fixed* (stability) axes, abbreviated EFS and BFS. DCFoil assumes an equilibrium state is provided (such as from a VPP).

6.1 Governing equations

The BFS and EFS origin is at the center of mass of the craft. Forward is x, port is y, and up is z. These are different axes from the foil. There are six degrees of freedom in the BFS $\boldsymbol{\eta} = [\eta_1, \eta_2, \eta_3, \eta_4, \eta_5, \eta_6]^T$. The six velocities in BFS are $[v_x, v_y, v_z, \omega_x, \omega_y, \omega_z]^T$ where the first three are $\mathbf{v}_B$ and the last three are $\boldsymbol{\omega}_B$. The orientation in EFS are *Euler angles* $[\phi, \theta, \psi]$. See Figure 2.

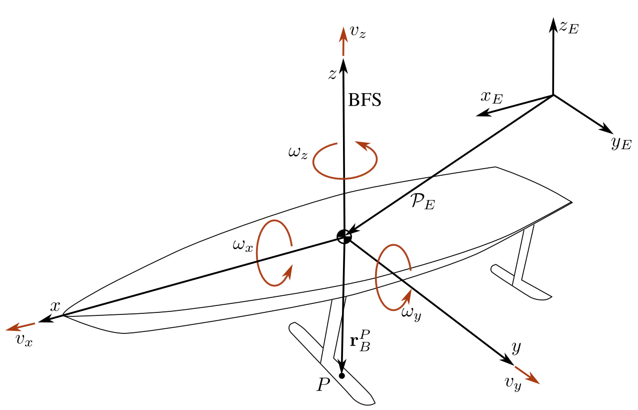

Figure 2: Coordinate system and degrees of freedom

6.2 Kinematics

A quantity of interest is the vessel velocity in the EFS denoted $\mathbf{v}_E$. Using Euler angles (from EFS obviously), the relationship between BFS and EFS center of mass velocity is

$$\mathbf{v}_E = \mathbf{R}_{BE}\mathbf{v}_B.$$

Now for some point P on the vessel not at the center of mass, the velocity is

$$\mathbf{v}_E^P = \dot{\mathcal{P}}_E + \dot{\mathbf{r}}_E^P = \mathbf{v}_E + \underbrace{\dot{\mathbf{r}}_E^P}_{\dot{\mathbf{R}}_{BE}\mathbf{r}_B^P},$$

where ship velocity is $\mathbf{v}_E = \dot{\mathcal{P}}_E$. The orientation of the ship in EFS is

$$\boxed{\begin{Bmatrix} \dot{\phi} \\ \dot{\theta} \\ \dot{\psi} \end{Bmatrix} = \mathbf{T}^{-1}\boldsymbol{\omega}_B = \begin{bmatrix} 1 & \sin\phi\tan\theta & \cos\phi\tan\theta \\ 0 & \cos\phi & -\sin\phi \\ 0 & \sin\phi\sec\theta & \cos\phi\sec\theta \end{bmatrix} \begin{Bmatrix} \omega_x \\ \omega_y \\ \omega_z \end{Bmatrix}}. \tag{42}$$

This is the equation you would plug into the time integration scheme. The *tangential operator* $\mathbf{T}(\phi, \theta, \psi)$ based on Euler angles is

$$\mathbf{T}(\phi, \theta, \psi) = \begin{bmatrix} 1 & 0 & -\sin\theta \\ 0 & \cos\phi & \sin\phi\cos\theta \\ 0 & -\sin\phi & \cos\phi\cos\theta \end{bmatrix}.$$

We wrote it this way to not use Euler angles. Finally, the *transport theorem* is

$$\mathbf{R}_{BE}\dot{\mathbf{v}}_E = \dot{\mathbf{v}}_B + \tilde{\omega}_B\mathbf{v}_B$$

where

$$\mathbf{R}_{BE}\dot{\mathbf{R}}_{EB} = \tilde{\omega}_B = \begin{bmatrix} 0 & -\omega_z & \omega_y \\ \omega_z & 0 & -\omega_x \\ -\omega_y & \omega_x & 0 \end{bmatrix}.$$

6.3 Inertia

Total linear momentum is

$$\mathbf{p}_B = \int_{\mathcal{V}} \mathbf{v}_B^P \, \mathrm{d}m = m\mathbf{v}_B$$

and the total angular momentum about the center of mass is

$$\mathbf{h}_B = \int_{\mathcal{V}} \tilde{\mathbf{r}}_B^P \mathbf{v}_B^P \, \mathrm{d}m = \mathbf{I}_B\boldsymbol{\omega}_B$$

where

$$\mathbf{I}_B = -\int_{\mathcal{V}} \tilde{\mathbf{r}}_B^P \tilde{\mathbf{r}}_B^P \, \mathrm{d}m = \begin{bmatrix} I_{xx} & -I_{xy} & -I_{xz} \\ -I_{yx} & I_{yy} & -I_{yz} \\ -I_{zx} & -I_{zy} & I_{zz} \end{bmatrix}$$

and $I_{xy} = I_{zy} = 0$ for P/S symmetry. Example quantities are $I_{xx} = \int_{\mathcal{V}} \left(y^2 + z^2\right) dm$ and $I_{yz} = I_{zy} = \int_{\mathcal{V}} yz dm$ In EFS, angular momentum is

$$\mathbf{h}_E = \mathbf{R}_{EB}\mathbf{h}_B = \underbrace{\mathbf{R}_{EB}\mathbf{I}_B\mathbf{R}_{BE}}_{\mathbf{I}_E}\,\omega_E$$

6.4 Equations of motion

If we plug into Lagrange's equations, we get the equations of motion in BFS

$$m\dot{\mathbf{v}}_B + m\tilde{\omega}_B\mathbf{v}_B = \mathbf{f}_{\mathrm{h}B} + \mathbf{f}_{pB} + \mathbf{f}_{gB} \tag{43}$$
$$\mathbf{I}_B\dot{\omega}_B + \tilde{\omega}_B\mathbf{I}_B\omega_B = \mathbf{m}_{aB} + \mathbf{m}_{pB} \tag{44}$$

where the RHS are hydrodynamic, propulsive, and gravitational loads acting on the center of mass.

6.4.1 Gravitational loads

The gravitational loads have explicit dependence on vehicle orientation.

$$\mathbf{f}_{gB} = mg\mathbf{R}_{BE}\mathbf{e}_3 = \left\{ \begin{array}{c} -mg\sin\theta \\ mg\cos\theta\sin\phi \\ mg\cos\theta\cos\phi \end{array} \right\}$$

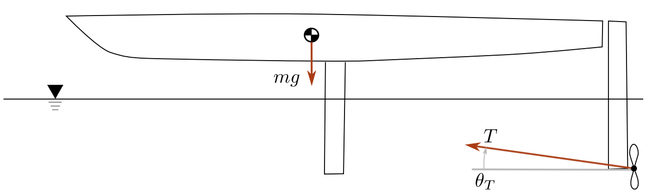

Figure 3: Gravitational and propulsive loads.

6.4.2 Propulsive forces

Assume the propulsion system acts at a point at $(x_T, 0, z_T)$ from the CM with some rake angle θ_T. The propulsive loads are then

$$\mathbf{f}_{pB} = \left\{ \begin{array}{c} T\cos\theta_T \\ 0 \\ -T\sin\theta_T \end{array} \right\}, \quad \mathbf{m}_{pB} = \left\{ \begin{array}{c} 0 \\ T\left(z_T\cos\theta_T + x_T\sin\theta_T\right) \\ 0 \end{array} \right\}$$

6.4.3 Hydrodynamic loads

The craft instantaneous angle of attack is

$$\alpha(t) = \tan^{-1}\frac{v_z(t) - v_{gz}(t)}{v_x(t) - v_{gx}(t)} \quad \text{and} \quad -\pi \le \alpha \le \pi$$

where $\mathbf{w} = -[v_{gx}, v_{gy}, v_{gz}, \omega_{gx}, \omega_{gy}, \omega_{gz}]^T$ is the disturbance vector of gusts (assume constant). Leeway angle is

$$\beta = \tan^{-1}\frac{v_y - v_{gy}}{\sqrt{\left(v_x - v_{gx}\right)^2 + \left(v_z - v_{gz}\right)^2}} \quad \text{and} \quad -\frac{\pi}{2} \le \beta \le \frac{\pi}{2}.$$

Finally, the velocity vector is

$$\mathbf{v}_B - \mathbf{v}_{gB} = \left\{ \begin{array}{c} v_x - v_{gx} \\ v_y - v_{gy} \\ v_z - v_{gz} \end{array} \right\} = V_{\mathrm{TAS}} \left\{ \begin{array}{c} \cos\alpha\cos\beta \\ -\sin\beta \\ \sin\alpha\cos\beta \end{array} \right\}$$

where $V_{TAS} = ||\mathbf{v}_B - \mathbf{v}_{gB}||$ is the magnitude of the true foiling speed.

$$\mathbf{f}_{aB} = \frac{1}{2}\rho V_{\mathrm{TAS}}^2 S\mathbf{c}_{\mathbf{f}_B}\left(\mathbf{v}_B - \mathbf{v}_{gB}, \omega_B - \omega_{gB}, \boldsymbol{\delta}_c; \sigma, \mathrm{Re}\right),$$
$$\mathbf{m}_{aB} = \frac{1}{2}\rho V_{\mathrm{TAS}}^2 S\boldsymbol{\Lambda}_{\mathrm{ref}}\mathbf{c}_{\mathbf{m}_B}\left(\mathbf{v}_B - \mathbf{v}_{gB}, \omega_B - \omega_{gB}, \boldsymbol{\delta}_c; \sigma, \mathrm{Re}\right),$$

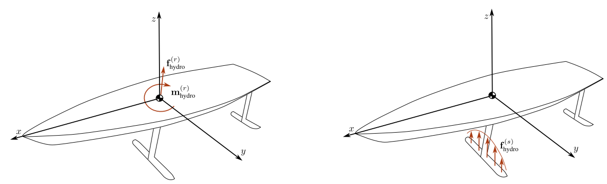

Figure 4: Hydrodynamic loads.

6.4.4 Elastified equations of motion

Defining the state vector as $\mathbf{x}_r(t) = [v_x, v_y, v_z, \omega_x, \omega_y, \omega_z, \phi, \theta]^T$ and the control inputs as $\mathbf{u} = [\delta_e, \delta_r]^T$ where δ_e and δ_r are elevator (main foil rake) and rudder command inputs, the dynamics of the system are

$$\dot{\mathbf{x}}_r = f^{(r)}(\mathbf{x}_r, \mathbf{x}_s, \mathbf{u}, \mathbf{w}) = \tag{45}$$
$$f_{\mathrm{gyr}}^{(r)}(\mathbf{x}_r) + f_{\mathrm{grav}}(\mathbf{x}_r) + f_{\mathrm{hydro}}^{(r)}(\mathbf{x}_r, \mathbf{x}_s, \mathbf{u}) + f_{\mathrm{prop}}^{(r)}(\mathbf{x}_r, \mathbf{x}_s, \mathbf{u}) \tag{46}$$

and (under the small amplitude structural deformation assumption) the deformations are determined by

$$\mathbf{K}_{ss}\mathbf{x}_s = f^{(s)}(\mathbf{x}_r, \mathbf{x}_\mathbf{s}, \mathbf{u}) = \tag{47}$$
$$f_{\mathrm{gyr}}^{(s)}(\mathbf{x}_r) + f_{\mathrm{grav}}(\mathbf{x}_r) + f_{\mathrm{hydro}}^{(s)}(\mathbf{x}_r, \mathbf{x}_s, \mathbf{u}) + f_{\mathrm{prop}}^{(s)}(\mathbf{x}_r, \mathbf{x}_s, \mathbf{u}) \tag{48}$$

where $\mathbf{x}_s(t)$ is the structural state vector.

Equations (45) and (47) are coupled and must be solved simultaneously. Static trim is $\mathbf{x}_{s0}$ and $\mathbf{x}_{r0}$. We solve the coupled system

$$f^{(r)}(\mathbf{x}_{s0}, \mathbf{x}_{r0}, \mathbf{u}_0) = \mathbf{0} \tag{49}$$
$$f^{(s)}(\mathbf{x}_{s0}, \mathbf{x}_{r0}, \mathbf{u}_0) = \mathbf{K}_{ss}\mathbf{x}_{s0} \tag{50}$$

Assuming small perturbations around the trimmed flight condition, the force Equations (45) and (47) can be linearized to

$$\Delta\dot{\mathbf{x}}_r = \mathbf{A}_{rr}\Delta\mathbf{x}_r + \mathbf{A}_{rs}\Delta\mathbf{x}_s + \mathbf{B}_r\Delta\mathbf{u}$$
$$\mathbf{K}_{ss}\Delta\mathbf{x}_s = \mathbf{A}_{sr}\Delta\mathbf{x}_r + \mathbf{A}_{ss}\Delta\mathbf{x}_s + \mathbf{B}_s\Delta\mathbf{u}$$

where the state ($\mathbf{A}$) and input ($\mathbf{B}$) matrices are partitions of the Jacobian of nonlinear forcing terms. This coupled system is linear so we can first solve for

$$\Delta\mathbf{x}_s = \left(\mathbf{K}_{ss} - \mathbf{A}_{ss}\right)^{-1}\left(\mathbf{A}_{sr}\Delta\mathbf{x}_r + \mathbf{B}_s\Delta\mathbf{u}\right)$$

and this is substituted back into the linearized coupled equations. The structural effects are a constant feedback on the rigid equations.

Now in the vibrating mode, if we assume small-amplitude vibrations, we must consider the shift of vehicle center of mass and its impact on the vehicle dynamics. If the elastic deformations are sufficiently small to not change global inertial characteristics, then modal coordinates can be used.

References

[1] Terrence A Weisshaar and Brian L Foist. Vibration tailoring of advanced composite lifting surfaces. *Journal of Aircraft*, 22(2):141–147, 1985.

[2] I. Lottati. Flutter and divergence aeroelastic characteristics for composite forward swept cantilevered wing. *Journal of Aircraft*, 22(11):1001–1007, nov 1985. doi: 10.2514/3.45238.

[3] H. Glauert. *The Elements of Aerofoil and Airscrew Theory*. Cambridge Science Classics. Cambridge University Press. doi: 10.1017/CBO9780511574481.

[4] Justin E Kerwin and Jacques B Hadler. Principles of naval architecture series: Propulsion. *The Society of Naval Architects and Marine Engineers (SNAME)*, pages 18–30, 2010.

[5] T. Theodorsen. General theory of aerodynamic instability and the mechanism of flutter. Technical Report Rept. 496, NACA, May 1934.

[6] Louw H. van Zyl. Aeroelastic divergence and aerodynamic lag roots. *Journal of Aircraft*, 38(3):586–588, May 2001. ISSN 0021-8669. doi: 10.2514/2.2806. URL `http://dx.doi.org/10.2514/2.2806`.

[7] Eirikur Jonsson. *High-fidelity Aerostructural Optimization of Flexible Wings with Flutter Constraints*. PhD thesis, University of Michigan, 2020.

[8] Eirikur Jonsson, Charles A. Mader, Graeme J. Kennedy, and Joaquim R. R. A. Martins. Computational modeling of flutter constraint for high-fidelity aerostructural optimization. In *2019 AIAA/ASCE/AHS/ASC Structures, Structural Dynamics, and Materials Conference*, San Diego, CA, January 2019. American Institute of Aeronautics and Astronautics. doi: 10.2514/6.2019-2354.

[9] Louw H. van Zyl. Use of eigenvectors in the solution of the flutter equation. *Journal of Aircraft*, 30(4):553–554, July 1993. ISSN 0021-8669. doi: 10.2514/3.46380. URL `http://dx.doi.org/10.2514/3.46380`.

[10] Eirikur Jonsson, Gaetan K. W. Kenway, Graeme J. Kennedy, and Joaquim R. R. A. Martins. Development of flutter constraints for high-fidelity aerostructural optimization. In *18th AIAA/ISSMO Multidisciplinary Analysis and Optimization Conference*, Denver, CO, June 2017. AIAA 2017-4455.